













Selective recognition of bisphenol S isomers in water by β -cyclodextrin

Ilaria Quaratesi , Paolo Della Sala , Clotilde Capacchione , Carmen Talotta , Silvano Geremia , Neal Hickey , Rocco Gliubizzi , Immacolata Bruno , Carmelo Sgarlata , Rossella Migliore , Carmine Gaeta , and Placido Neri 

^aDipartimento di Chimica E Biologia "A. Zambelli", Università di Salerno, Fisciano, Italy; ^bBi-qemrties Spa, Zona Industriale - Buccino, Italy; ^cCentro di Eccellenza in Biocristallografia, Dipartimento di Scienze Chimiche E Farmaceutiche, Università di Trieste, Trieste, Italy; ^dDipartimento di Scienze Chimiche, Università Degli Studi Di Catania, Catania, Italy; ^eIstituto di Chimica Biomolecolare, Consiglio Nazionale Delle Ricerche, Catania, Italy

ABSTRACT

The two isomers 4,4'-dihydroxydiphenyl sulphone and 2,4'-dihydroxydiphenyl sulphone (bisphenol S, **BPS**) form inclusion complexes with β -CD in solution, in the gas phase, and in the solid state. The complexes **4,4'-BPS@ β -CD** and **2,4'-BPS@ β -CD** were studied in solution by 1D and 2D NMR experiments. Calorimetric investigation by ITC evidenced that the β -CD host shows a greater affinity for **4,4'-BPS**, with a **4,4'-BPS/2,4'-BPS** selectivity ratio of 6.3. In the gas phase, CID MS experiments indicate that 4,4'-BPS has a higher kinetic barrier to escape from the β -CD cavity than the isomeric 2,4'-BPS. In the solid state, the **4,4'-BPS@ β -CD** and **2,4'-BPS@ β -CD** complexes form head-to-head dimers constituted by two β -CD macrocycles, with each β -CD hosting one **BPS** guest. The dimers of β -CD are sealed by H-bonding interactions involving exclusively the secondary OH groups. Finally, the formation of inclusion complexes between **4,4'-BPS** or **2,4'-BPS** and β -CD was also followed by FT-IR, DSC, and TGA analysis.



Introduction

Molecular recognition of highly persistent organic pollutants has rapidly arisen as a major field of fundamental research in supramolecular chemistry [1–6]. Bisphenols [7] are a family of phenol-based building blocks widely used as additives for the synthesis of epoxy-resins and polycarbonates [7]. The most common member of this family is bisphenol A (BPA, Figure 1) which has been recently superseded by bisphenol S [8]. Bisphenol S (4,4'-BPS; 4,4'-dihydroxydiphenyl sulphone) was introduced as a safer alternative to BPA and its bisphenol-based plastics show excellent mechanical performance and thermal stability [9]. Unfortunately, due to the presence of the SO₂ group, the water-soluble bisphenol S shows high thermal stability and low photodegradation [9]. Therefore, it exhibits very high persistence in the

aqueous environment. In addition, BPS shows severe adverse effects on human health, such as oestrogenic activity and carcinogenicity [10–12]. Despite this, bisphenols are present in many everyday products, especially in baby formula packaging, baby bottles, and household food containers [13]. For these reasons, the United States Environmental Protection Agency (EPA) has classified bisphenols as the third priority class in terms of toxicity profile. Thus, in the last decades, many studies have been conducted on the removal of bisphenol as a pollutant [14–20]. In this context, cyclodextrins (CD) [21,22] could play a crucial role thanks to their molecular recognition abilities in aqueous solvent [14–20]; for example, it has been reported that the heptameric β -CD can form an inclusion complex in water with bisphenol S [17,18]. Recently, Helbling and Ditchel [15] reported a β -CD-based mesoporous polymer with

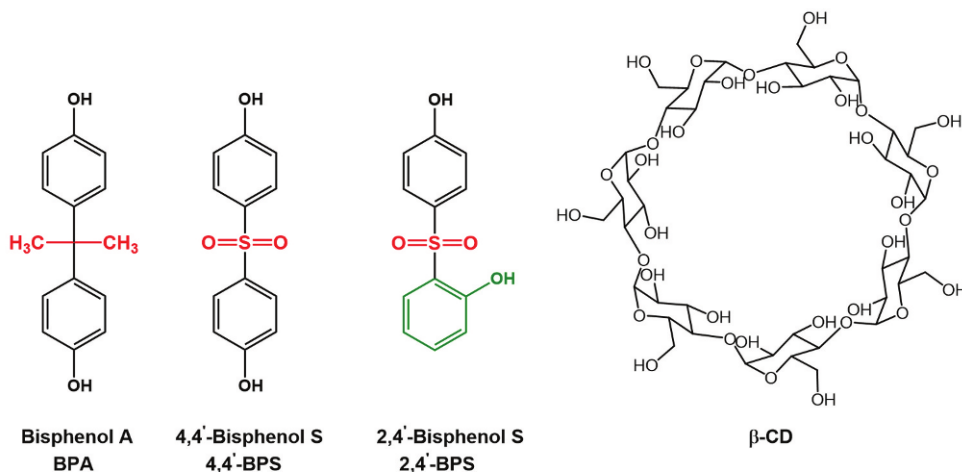


Figure 1. Chemical drawing of BPA, BPSs, and β -CD investigated in the present work.

a high surface area which rapidly sequesters bisphenol A and S from water, with adsorption rate constants up to 200 times greater than those of non-porous β -CD adsorbent materials.

During the synthesis of 4,4'-dihydroxydiphenyl sulphone (bisphenol S) large quantities of the isomeric 2,4'-dihydroxydiphenyl sulphone (2,4'-BPS) are formed as by-product [23]. Consequently, the commercial product known as bisphenol S is in fact a mixture of both isomeric dihydroxy diphenyl sulphones, as the purification of the pure bisphenol S (4,4'-isomer) from mixtures with the 2,4'-isomer cannot be easily achieved [23]. Unfortunately, the presence of the 2,4'-isomer complicates the application of bisphenol S, and increases the related pollution problems.

Molecular recognition [24] of constitutionally isomeric species is of practical interest [1–6,25], and this is particularly true for organic pollutants such as BPS isomers, which show very similar chemical and physical properties. Due to this similarity, it is difficult to separate them by employing commonly used methods like crystallisation or chromatography. Consequently, the study of supramolecular hosts able to discriminate between isomeric guests could pave the way to the construction of new materials for the economic separation and purification of the two isomeric 4,4'-and 2,4'-dihydroxydiphenyl sulphones. While many studies have been reported concerning the molecular recognition of 4,4'-dihydroxydiphenyl sulphone (bisphenol S) inside the hydrophobic cavity of β -CD in aqueous system [17,18]; to date, no information has been reported regarding the complexation abilities of β -CD towards the 2,4'-isomer in water.

Prompted by these considerations, in this study we have evaluated the complexation abilities of β -CD towards the two isomeric dihydroxydiphenyl sulphones, in solution, in the solid state, and in the gas phase.

Results and discussion

Complexation study of 4,4'-BPS and 2,4'-BPS in solution via 1D and 2D NMR

The complexation abilities of β -CD towards the two isomeric 4,4'-and 2,4'-dihydroxydiphenyl sulphones (Figure 1) were initially evaluated by ^1H NMR titration experiments (Figures 2 and 3) [26,27]. When the D_2O solution of β -CD was titrated with 4,4'-dihydroxydiphenyl sulphone (4,4'-BPS), substantial changes were observed in their respective ^1H NMR signals, indicative of the formation of the 4,4'-BPS@ β -CD complex (Figure 2a–c). Under these conditions, a single set of averaged ^1H NMR signals (Figure 2b) for both β -CD host and 4,4'-BPS guest was observed, indicating a fast exchange equilibrium between free and bound species on the NMR timescale. In a 1:1 mixture of β -CD host and 4,4'-BPS in D_2O , a significant up-field shift of -0.42 ppm for the H5-atom of β -CD located inside the cavity was observed, while smaller shifts for H2, H3, and H6 of -0.07 , -0.15 , and -0.15 ppm were observed, respectively. Analogously, a shift was also observed for the aromatic H-atoms of 4,4'-BPS upon inclusion inside the β -CD cavity. Thus, the H1^G and H2^G (Figure 2) H-atoms were up-field shifted by -0.04 and -0.10 ppm, respectively. 2D NOESY spectra (Figure 2f) confirmed the inclusion of 4,4'-BPS inside the cavity of β -CD. In fact, diagnostic dipolar couplings were observed between the aromatic H1^G (in *ortho* to OH group) of

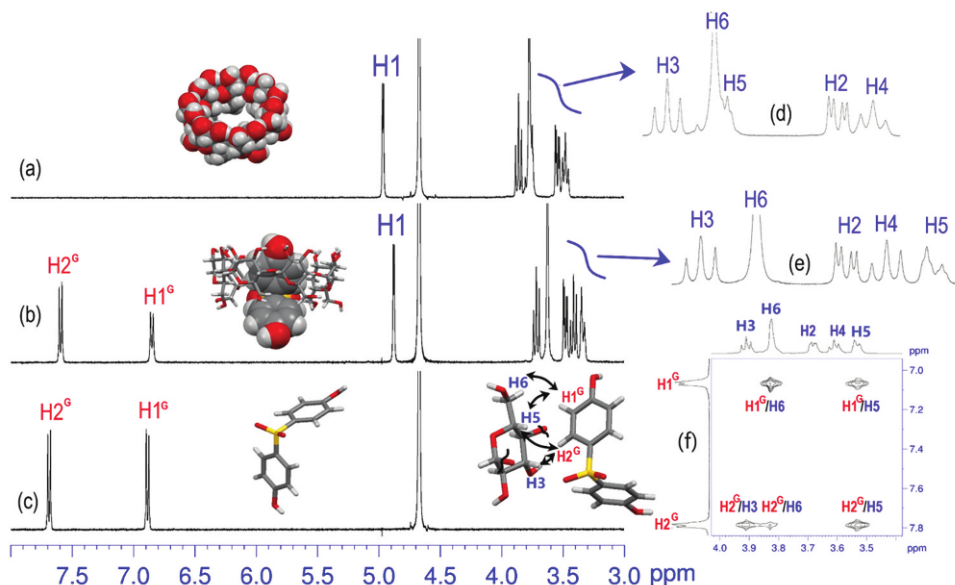


Figure 2. (a-e) ^1H NMR spectra (400 MHz, 298 K, D_2O) of: a) β -CD; b) Equimolar mixture of β -CD and 4,4'-BPS (3.0 mM); c) 4,4'-BPS; d) Expansion from 3.0 to 4.0 ppm of the ^1H NMR spectrum of β -CD in (a); e) Expansion from 3.0 to 4.0 ppm of the ^1H NMR spectrum of the 4,4'-BPS@ β -CD complex in (b); f) Most relevant portion of the 2D NOESY spectrum of the 4,4'-BPS@ β -CD complex. In (b) the solid-state structure of the 4,4'-BPS@ β -CD complex is reported (*vide infra*).

4,4'-BPS guest and the H6 and H5 atoms of β -CD, while the aromatic H2^G (in *meta* to OH group) of the guest showed dipolar couplings with the H3 and H5 atoms of β -CD.

In sharp contrast, the H2 and H4 atoms of β -CD, which are located outside the cavity, do not show dipolar couplings with the guest. The presence of dipolar couplings (Figure 2f) between the aromatic H-atoms of

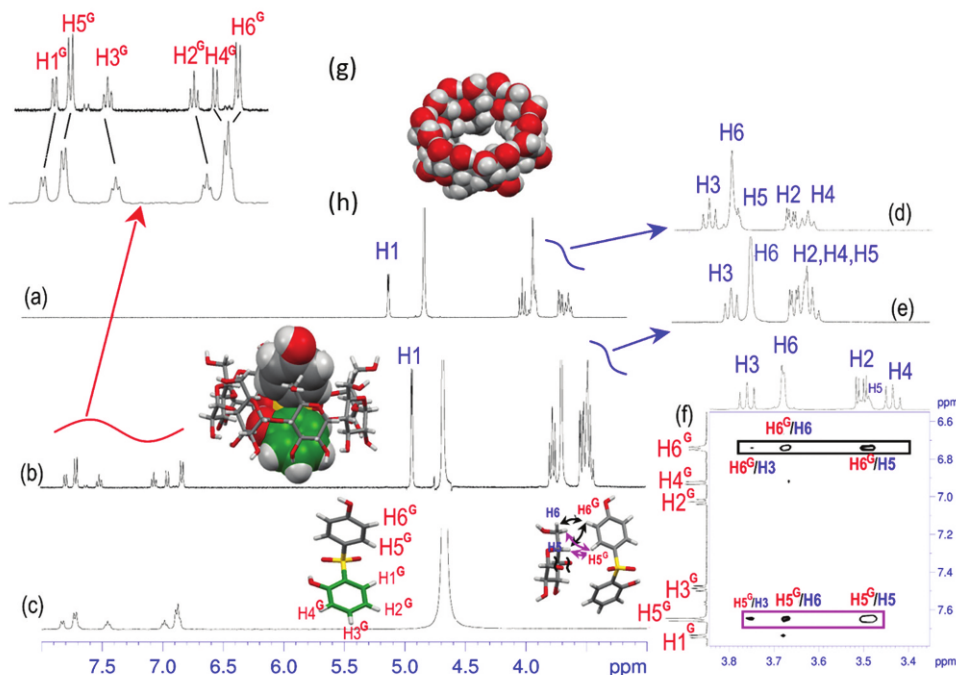


Figure 3. (a-c) ^1H NMR spectra (600 MHz, 298 K, D_2O) of: a) β -CD; b) Equimolar mixture of β -CD and 2,4'-BPS (3.0 mM); c) 2,4'-BPS; d) Expansion from 3.0 to 4.0 ppm of the ^1H NMR spectrum of β -CD in (a); e) Expansion from 3.0 to 4.0 ppm of the ^1H NMR spectrum of the 2,4'-BPS@ β -CD complex in (b); f) Most relevant portion of the 2D NOESY spectrum of the 2,4'-BPS@ β -CD complex; g) Expansion from 6.5 to 8.0 ppm of the ^1H NMR spectrum of the 2,4'-BPS@ β -CD complex in (b); h) Expansion from 6.5 to 8.0 ppm of the ^1H NMR spectrum of the 2,4'-BPS in (c). In (b) the solid state structure of the 2,4'-BPS@ β -CD complex is reported (*vide infra*).

the **4,4'-BPS** guest and the H5 and H6 (CH₂OH) atoms of the **β-CD** host clearly indicates the proximity of the guest with the primary face of **β-CD**.

Analogously, when a D₂O solution of **β-CD** was added to **2,4'-BPS**, an up-field shift of the ¹H NMR signals of the **β-CD** host was observed (Figure 3a-e), with typical shifts of -0.1 (H3), -0.1 (H6), -0.27 (H5) ppm. Similar shifts were observed in the ¹H NMR signals of **2,4'-BPS** guest. In detail, H1, H5, and H6 were up-field shifted, while H2, H3, and H4 were down-field shifted. Under these conditions, a single set of averaged ¹H NMR signals for both host and guest was observed, indicating a fast exchange between free and bound species on the NMR timescale. Interestingly, a 2D NOESY spectrum (Figure 3f) evidenced the presence of strong dipolar couplings between H5, H3 and H6-atoms on the inner cavity of **β-CD** and H5^G and H6^G aromatic atoms of the 4'-phenol unit of **2,4'-BPS** guest. In contrast, the 2-phenol unit of **2,4'-BPS** did not show significant dipolar couplings with the H-atoms of **β-CD**. These results suggest a probable structure of the **2,4'-BPS@β-CD** complex in which the 4'-phenol unit is included inside the cavity of the **β-CD**, while the 2-phenol unit is outside the cavity.

Diffusion-Ordered Spectroscopy (DOSY) NMR [28,29] is a useful tool for the study of host-guest complexation processes [26,27]. Thus, we performed DOSY NMR measurements to study the stoichiometry [29] of the **2,4'-BPS@β-CD** complex. Analysis of the DOSY spectrum (SI) of a 1:1 mixture of **2,4'-BPS** and **β-CD** in D₂O (298 K, 2.66 mM) provided a diffusion coefficient of $2.88 \pm 0.05 \times 10^{-10} \text{ m}^2/\text{s}$ for the complex **2,4'-BPS** (Table S4), significantly lower than that of free **2,4'-BPS** under the same conditions ($4.88 \pm 0.04 \times 10^{-10} \text{ m}^2/\text{s}$) (SI) but similar to that of free **β-CD** ($2.70 \pm 0.03 \times 10^{-10} \text{ m}^2/\text{s}$) [30-33]. This result strongly corroborates the formation of a stable inclusion complex between **β-CD** and **2,4'-BPS** in which the guest diffuses more slowly than in the free state [28].

The ratio of the diffusion coefficients for two different molecular species is inversely proportional to the cube-root of the ratio of their molecular masses for spherical molecules [27]. Based on this relationship, the diffusion coefficients measured for the complex **2,4'-BPS** and free **2,4'-**

BPS were consistent with a 1:1 stoichiometry of the **2,4'-BPS@β-CD** complex. An analogous DOSY study was performed for the 1:1 mixture of **4,4'-BPS/β-CD** (2.66 mM, 298 K, D₂O), and provided a diffusion coefficient of $2.95 \pm 0.05 \times 10^{-10} \text{ m}^2/\text{s}$ for the complex **4,4'-BPS** (Table S3). The results indicated a 1:1 stoichiometry of the **4,4'-BPS@β-CD** complex also in this case. Finally, Job's plot experiments (SI) confirmed the 1:1 host/guest ratio for the complexes **BPS@β-CD** in solution.

Complexation study of **4,4'-BPS** and **2,4'-BPS** in the gas phase by FT ICR MS investigation

Gas phase MS is a useful tool to study the structure of inclusion complexes without the complicating effect of solvent molecules [34-37]. In this way, it is possible to gain insights on specific host-guest interactions. In fact, the main stabilising effect of **β-CD**-inclusion complexes in solution is the so-called 'hydrophobic effect' [21,22], in which the liberation of 'high-energy' water from the cyclodextrin cavity after the inclusion of a guest plays a crucial role [21,22]. Clearly, in the gas phase, the 'hydrophobic effect' is absent and consequently the stability of the **β-CD**-complex is strongly affected. In fact, the literature data [33,35,36] show that some **β-CD**-inclusion complexes are not observed in the gas phase even if they are present in solution.

The HR ESI-FT-ICR mass spectrum of a 1:1 mixture of **4,4'-BPS** and **β-CD** in water showed a molecular ion peak at m/z 715.1881 (Figure 4) in agreement with the molecular formula of the complex [**4,4'-BPS@β-CD** + 2Na]²⁺ (calcd for C₅₄H₈₀Na₂O₃₉S, 715.1891). Analogously, the formation of the **2,4'-BPS@β-CD** complex in the gas phase was confirmed by the HR ESI-FT-ICR mass spectrum of a 1:1 mixture of **2,4'-BPS** and **β-CD** in water, which showed a molecular ion peak at m/z 715.1887 (Figure 4) in agreement with the molecular formula of the complex [**2,4'-BPS@β-CD** + 2Na]²⁺ (calcd for C₅₄H₈₀Na₂O₃₉S, 715.1891). In conclusion, the detection of inclusion complexes **2,4'-BPS@β-CD** and **4,4'-BPS@β-CD** suggests the high stability of these supramolecular complexes in the gas phase (*vide infra*: ITC, FT IR studies).

It is known that, in the gas phase, the supramolecular guest@host complex ions are associated until they are energetically activated by collision with neutral reagent gases [34,35,38]. Collision-induced dissociation experiments of supramolecular complexes in the gas phase offer useful insight on activation energies for the guest@host dissociation processes [34,39]. Thus, in order to confirm the inclusion of **4,4'-BPS** and **2,4'-BPS** inside the cavity of **β-CD**, we performed an ESI-CID MS/MS experiment (Figure 4). The CID mass spectra of the sodium adducts of **4,4'-BPS@β-CD** and **2,4'-BPS@β-CD** are shown in Figures 4a and 4b, respectively, and are in agreement with the loss of the BPS guest due to its release from the **β-CD** cavity. The collision-induced dissociation of the BPS@β-CD complexes were studied at different acceleration voltages, and consequently at different average collision energies. A lower energy is required to dissociate supramolecular complexes with respect to the fragmentation of molecules due to rupture of covalent bonds [33,35,36,38].

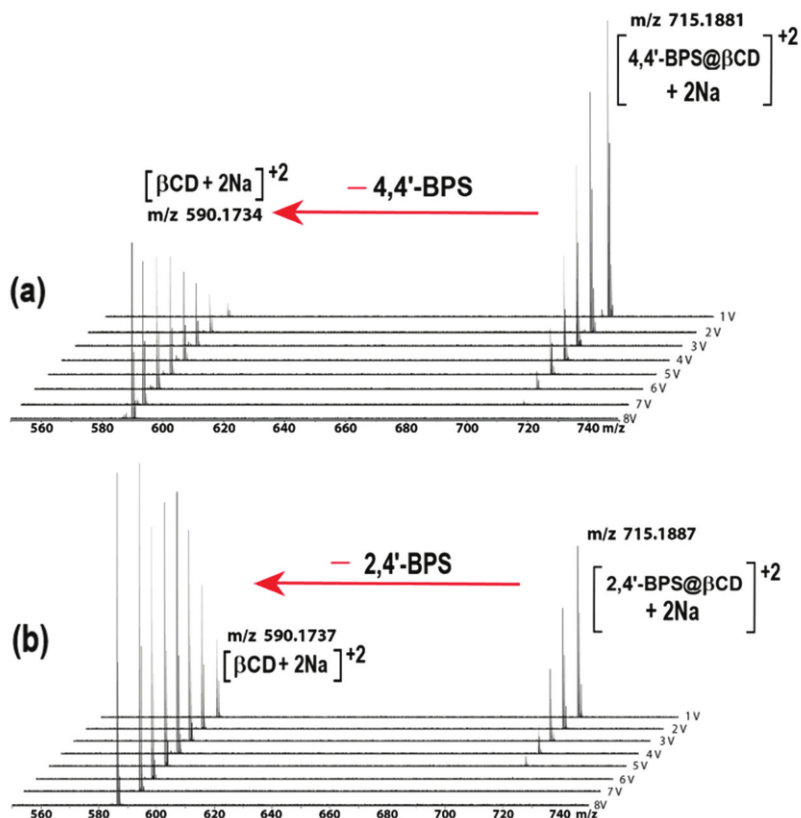


Figure 4. Series of ESI FT ICR CID mass spectra of: (a) 1:1 mixture of β -CD and **4,4'-BPS**; and (b) 1:1 mixture of β -CD and **2,4'-BPS**. After collisions with argon at acceleration voltages of 1–8 V.

Regarding the **2,4'-BPS@ β -CD** complex, already at a low voltage of 1 V, the intensity ratio $I_{(2,4'-BPS@ \beta-CD)}/I_{(\beta-CD)}$ is 2/1, while the MS/MS spectrum of **4,4'-BPS@ β -CD** (Figure 4a) shows an intensity ratio $I_{(4,4'-BPS@ \beta-CD)}/I_{(\beta-CD)}$ of 20/1. Analogously, across the range 2–6 V the intensity ratio $I_{(4,4'-BPS@ \beta-CD)}/I_{(\beta-CD)}$ is more than 10 times larger than the analogous intensity ratio of the isomeric **2,4'-BPS@ β -CD** complex. This result suggests that **4,4'-BPS** has a higher kinetic barrier to escape from the β -CD cavity than the isomeric **2,4'-BPS** [39].

Complexation study of 4,4'-BPS and 2,4'-BPS in the solid state

A detailed solid-state study [40] has been previously reported regarding inclusion complexes between β -CD and bisphenol A (BPA) (Figure 5e,f), while to the best of our knowledge, no information is present in the literature regarding the solid state structures of the **4,4'-BPS** or **2,4'-BPS** inclusion complexes with β -CD. The **4,4'-BPS@ β -CD** complex (Figure 5a,b) crystallises in the orthorhombic system (space group $P2_12_12_1$). The asymmetric unit consists of a common head-to-head dimer formed by two β -CD macrocycles, which hosts two **4,4'-**

BPS guests (Figure 5a). In addition, a total of 27.7 water molecules were refined in 42 crystallographically independent sites. The **4,4'-BPS** guest molecules were refined with a two-position disorder (occupancy factors 0.8/0.2) and a three-position disorder (occupancy factors 0.5/0.3/0.2).

The β -CD macrocycles show the typical chair conformation of the glucose units with an overall pseudo C_7 point symmetry (Figure 5b). The secondary O2 and O3 hydroxyl groups of each molecule constitute the interface of the dimer (Figure 5a). As previously reported [41], due to the geometry of the O2 and O3 configurations, only the O3 hydroxyl hydrogens can be orientated directly towards a facing O3 oxygen atom. Therefore, two β -CD units are sealed by seven strong H-bonding interactions involving exclusively the secondary O3 hydroxyl groups of the two β -CD units, with an average O...O distance of 2.82 Å and an average O–H...O angle of 169° (Figure 5a). Furthermore, a water molecule bridges the two β -CDs (Figure 5a) donating a single hydrogen bond (O–H...O distance of 2.80 Å and an O–H...O angle of 124°) and accepting a single hydrogen-bond (O–H...O distance of 2.68 Å and an O–H...O angle of 164°). The distance between the two barycenters of the almost

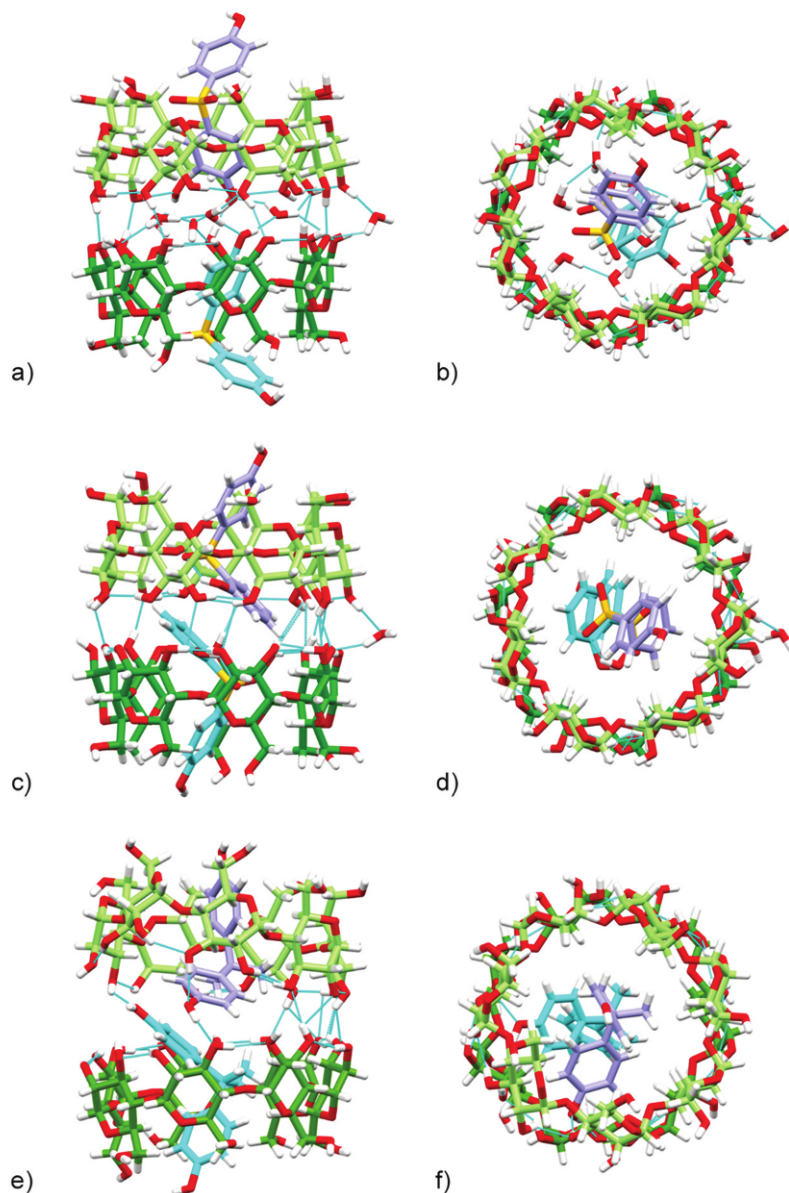


Figure 5. Side and top views of the solid state of bisphenol@ β -CD dimeric complexes: (a, b) $(4,4'\text{-BPS@ } \beta\text{-CD})_2$; (c, d) $(2,4'\text{-BPS@ } \beta\text{-CD})_2$; (e, f) $(\text{BPA@ } \beta\text{-CD})_2$ [40]; Different colours of C-atoms are used to distinguish the different molecules. H-bonds are indicated by dashed lines. For clarity, only the conformation of the guest molecules with highest occupancy are shown.

regular heptagons described by the O4 glycosidic atoms (Table S2) is 6.933 Å. The two β -CD are mutually rotated by about 10° (Figure 5b).

Interestingly, at the interface of the dimer $(4,4'\text{-BPS@ } \beta\text{-CD})_2$ five water molecules were found. These form a hydrogen-bonded network (Figure 5a,b) which also involves two phenolic groups of the $4,4'\text{-BPS}$ guests. This encapsulated network of water molecules contributed to stabilise the dimeric $(4,4'\text{-BPS@ } \beta\text{-CD})_2$ structure in the solid state (Figure 5a,b). To simplify the description of the host-guest interactions, only the conformation of the disordered guest with highest occupancy will be discussed. The two-independent $4,4'\text{-BPS}$ units are

inserted into the macrocycles in a similar way with one phenolic group exposed outside the β -CDs (Figure 5a). In fact, the central sulphur atoms are 2.526 and 2.619 Å out of the respective planes defined by the O4 glycosidic atoms (Figure 5a). The dihedral angles between the phenolic planes and the respective O4 glycosidic planes are 59.1° and 59.5° for the internal and 39.1° and 46.2° for the external phenolic groups. This clearly indicates the similarity of the two host-guest conformations with a mutual rotation of the two guest molecules of 105° (Figure 5b). No direct strong H-bonds are observed between host and guest, including the sulphone group. However, the internal phenolic group is located

in the interface plane defined by the O2 and O3 atoms and it is involved in the network of H-bonds with the five water molecules sandwiched between the β -CD dimeric assembly (Figure 5a,b).

The **2,4'-BPS@ β -CD** complex (Figure 5c,d) crystallises in the triclinic system (space group P1). The asymmetric unit consists of a β -CD dimer, which hosts two **2,4'-BPS** guests (Figure 5c). In addition, a total of 21.4 water molecules were refined in 40 crystallographically independent sites. Both **2,4'-BPS** molecules were refined with a two-position disorder (occupancy factors 0.8/0.2), related by a pseudo-twofold rotation around the central axis of the dimer. Further, two-position disorder was observed for the *ortho* oxygen atoms of the phenolic groups with higher occupancy, related to a 180° rotation (occupancy factors 0.6/0.2 and 0.45/0.35). The **2,4'-BPS@ β -CD** complex also forms a head-to-head dimeric structure in the solid state (Figure 5c) in which two β -CD macrocycles are sealed by H-bonding interactions between the secondary OH functions (four strong O–H...O interactions involving the O3 hydroxyl groups with average distance of 2.79 Å and an average O–H...O angle of 156° and one much weaker intermolecular H-bond between O3 and O2 hydroxyl groups with a distance of 3.09 Å and an O–H...O angle of 123°). In addition, also in this case, a hydrogen-bonded bridge was detected between one water molecule and the two β -CDs (Figure 5c). The distance of 7.042 Å between the two barycenters of the almost regular heptagons described by the O4 glycosidic atoms is slightly longer than that observed for the **4,4'-BPS@ β -CD** complex, consistent with the smaller number of H-bond interactions sealing the dimer interface. The two independent **2,4'-BPS** guests are centrally inserted into the dimeric hosts in similar ways with both 2-phenolic units more internal to the dimer. The central sulphur atoms are –0.531 and –0.077 Å out of the respective planes defined by the O4 glycosidic atoms (the negative sign indicated an out-of-plane towards the internal of the dimer). Therefore, with respect to the **4,4'-BPS** the central sulphur atoms are more deeply inserted by up to 3.0 Å (Figure 5c). The dihedral angles between the phenolic planes and the respective O4 glycosidic planes are 43.6° and 45.5° for the 2-phenolic unit and 60.2° and 61.5° for the 4'-phenolic unit. This clearly indicates the similarity of the two host-guest conformation with a mutual rotation of the two guest molecules of 170° (Figure 5d). In this conformation, a π ... π interaction between the 2-phenol rings (centroid separation 3.85 Å) of the **2,4'-BPS** guests is formed (Figure 5c). No direct strong H-bonds are observed between host and guest, including the sulphone group and the 2-phenolic oxygen deeply inserted in the dimer. These groups are

involved in an intramolecular H-bond and in weak C–H...O interactions with the host molecule. No water molecules were detected at the dimer interface, in contrast to that observed in the case of the **4,4'-BPS** complex. This highlights the determining role of the phenolic oxygen in the 4-position, located in the dimer interface, for the organisation of the H-bond network with the sandwiched water molecules. The analogous **BPA@ β -CD** complex previously reported [41] also shows a similar dimer-like complex. However, the guest in this case is much more deeply inserted and off-centre (–1.366 and –0.524 Å out of plane distances of the central carbon atoms from the O4 glycosidic planes) and the internal 4-phenolic units partially interfere with the β -CD dimeric interface. In fact, in comparison to the complexes here reported, the two distances between the O4 glycosidic centroids increase to 7.783 Å and the β -CD units are no longer parallel, with a dihedral angle of 15° (Figure 5e,f).

Thermodynamic insights on the complexation of 4,4'-BPS and 2,4'-BPS in solution by ITC

Typical ITC titrations for **2,4'-BPS/ β -CD** and **4,4'-BPS/ β -CD** systems in neutral aqueous solution (pH 7, phosphate buffer) at 25°C are shown in Figures 6 and Figures 7, respectively. The binding equilibria and thermodynamic parameters for the complex formation are listed in Table 1.

Two different sets of titrations, exploring both small and large host-guest ratios, were carried out for each **BPS/ β -CD** system to determine the complex species formed in the solution. The first set of experiments was run essentially to quantitate the 1:1 species, whereas the second set was run to assess the possibility of further aggregation with formation of complexes with different stoichiometries. In order to avoid artefacts, the two sets of data were refined together to obtain the final values. Different species and combinations thereof were examined but the data analysis invariably converged on the species and values reported in Table 1, whilst rejecting all the other models.

Both BPS isomers form inclusion complexes with β -CD host although shape and size of the guests affect their binding features. The stability of the 1:1 complex depends on the position of the hydroxyl groups in the guest molecule and the presence of both OH groups in the *para* position (**4,4'-BPS**) yields an increase in the binding constant value (of about 0.8 log unit) and the formation of an additional 1:2 **4,4'-BPS@(β -CD)₂** complex species. We suppose that this latter adduct assumes a capsular-like arrangement with two β -CD units capping both ends of the guest [42,43].

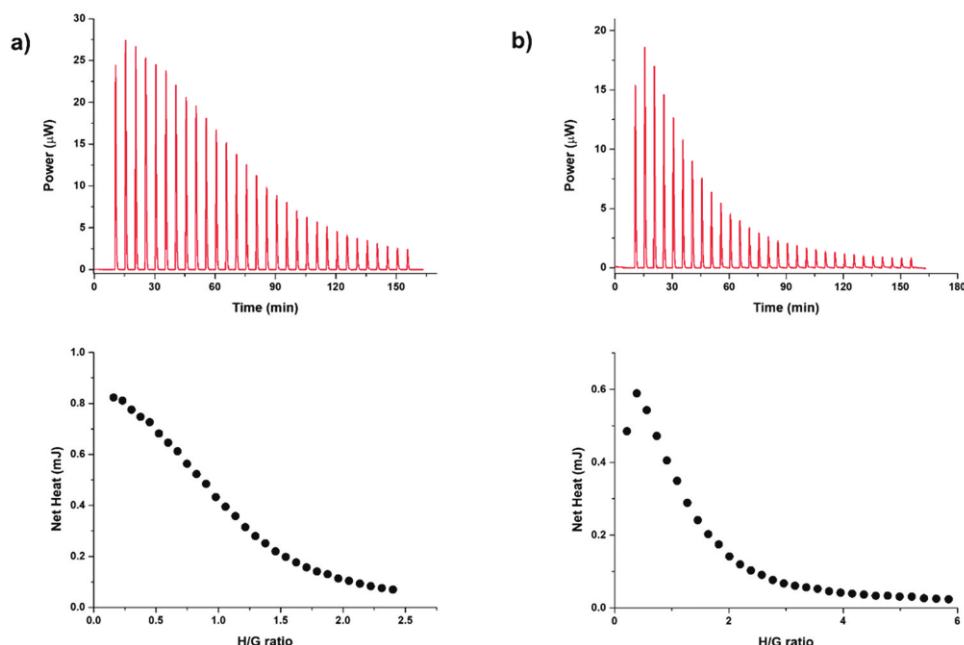


Figure 6. A) ITC titration curve of $\beta\text{-CD}$ (4 mM) into $4,4'\text{-BPS}$ (0.5 mM) at 25°C in aqueous solution (pH 7, phosphate buffer) with final H/G ratio of 2.5 (top) and integrated heat data (bottom); b) ITC titration curve of $\beta\text{-CD}$ (5 mM) into $4,4'\text{-BPS}$ (0.2 mM) at 25°C in aqueous solution (pH 7, phosphate buffer) with final H/G ratio of 6 (top) and integrated heat data (bottom) .

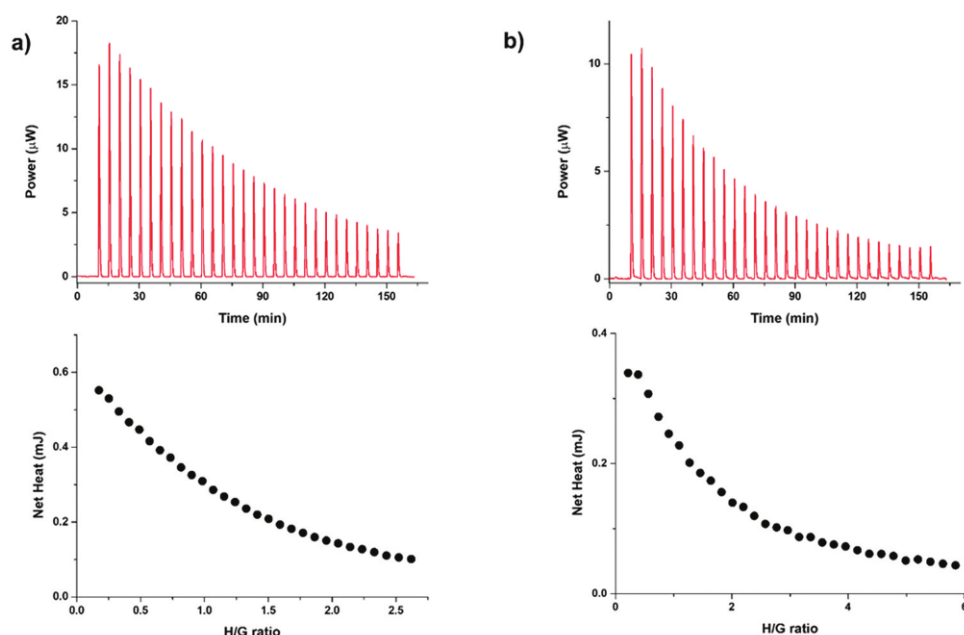


Figure 7. A) ITC titration curve of $\beta\text{-CD}$ (4 mM) into $2,4'\text{-BPS}$ (0.5 mM) at 25°C in aqueous solution (pH 7, phosphate buffer) with final H/G ratio of 2.6 (top) and integrated heat data (bottom); b) ITC titration curve of $\beta\text{-CD}$ (5 mM) into $2,4'\text{-BPS}$ (0.2 mM) at 25°C in aqueous solution (pH 7, phosphate buffer) with final H/G ratio of 6 (top) and integrated heat data (bottom) .

For both guests, the formation of the 1:1 species is driven by favourable enthalpy, but accompanied by an unfavourable entropy (Figure 8). A similar thermodynamic pattern has been reported previously for some inclusion complexes formed by cyclodextrins [44–48].

Weak non-covalent interactions, such as dipole–dipole and hydrogen bonding, drive the host–guest complex formation; these enthalpically favourable contributions override the energy cost needed for the desolvation of the interacting molecules. The unfavourable entropic term is the result of a balance between host

Table 1. LogK values and thermodynamic parameters for the formation of the **4,4'-BPS@ β -CD**, **4,4'-BPS@(β -CD)₂** and **2,4'-BPS@ β -CD** complexes at 25°C in neutral aqueous solution (pH 7, phosphate buffer 50 mM) .

Guest	Equilibrium	LogK	ΔH° (kJ mol ⁻¹)	ΔS° (J deg ⁻¹ mol ⁻¹)
4,4'-BPS	H + G HG	4.23 [9]	-28.72 [1]	-15.4 [12]
	HG + H H ₂ G	2.6 [7]	-9.44 [7]	18 [10]
2,4'-BPS	H + G HG	3.43 [1]	-32.57 [1]	-43.5 [1]

and guest desolvation ($\Delta S^\circ > 0$) and the loss of degrees of freedom due to the complex formation ($\Delta S^\circ < 0$), the latter being the prevalent contribution. This is a typical case in which the presence of a particular functional group in any of the binding partners improves the binding affinity by enthalpic factors (due to the presence of functions able to establish dipole-dipole or hydrogen bond interactions) which are counterbalanced by unfavourable entropic contribution (because of a loss in conformational degrees of freedom upon binding or a lower desolvation effect). Moreover, a favourable enthalpy contribution indicates that specific interactions are occurring between the binding partners and is an excellent way to ensure ligand specificity, selectivity, and adaptability [49]. In conclusion, ITC study clearly indicates that the β -CD host shows a greater affinity for **4,4'-BPS** with respect to its isomer **2,4'-BPS** with a **4,4'-BPS/2,4'-BPS** selectivity ratio of 6.3 (calculated as the ratio between the K values for the formation of 1:1 complexes in Table 1).

The formation of the complex **4,4'-BPS@(β -CD)₂**, (in Table 1, HG+H = H₂G), obtained at higher concentration of β -CD, is both enthalpically and entropically favoured. Indeed, the enthalpy gain resulting from additional interactions with the second β -CD cavity is mainly responsible for the formation of the complex along with a favourable entropic contribution.

DSC, TGA, and FT-IR analysis of the inclusion complexes 4,4'-BPS@ β -CD and 2,4'-BPS@ β -CD

It is known that DSC analysis is also useful to highlight the formation of β -CD inclusion complexes [50,51]. As a guest molecule is included into β -CD cavity, melting, boiling, and sublimation points are shifted to different temperatures or simply disappear [50,51]. As shown in Figure 9a, the thermogram of β -CD highlighted a broad endothermic peak ($T_{\max} = 106^\circ\text{C}$), attributable to the release of co-crystallised water molecules. The DSC curve of the **4,4'-BPS** showed a sharp endothermic peak ($T_{\max} = 248.3^\circ\text{C}$) associated to its melting event. At this point, a 1:1 mixture of β -CD/**4,4'-BPS** was prepared by stirring the two components in an aqueous solution at 25°C for 30 min, then the solvent was removed under reduced pressure by a rotary evaporator. The thermogram of the 1:1 mixture β -CD/**4,4'-BPS** in Figure 9c shows the absence of the above mentioned **4,4'-BPS** melting peak: this result clearly indicated its molecular encapsulation inside the β -CD cavity [50,51]. Regarding the behaviour of the β -CD, the thermogram of the 1:1 mixture β -CD/**4,4'-BPS** in Figure 9c shows the presence of a weak and broad transition from 80°C to 130°C, which would be associated to the release of residual water included inside the β -CD cavity or in the crystal packing. In addition, the DSC curve of the 2:1 mixture β -CD/**4,4'-BPS** shows a wide peak between 40°C and 120°C (Figure 9b), attributable to water release from free β -

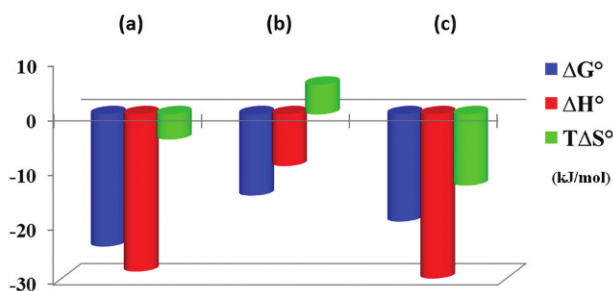


Figure 8. Thermodynamic parameters for the formation of complexes: (a) **4,4'-BPS@ β -CD**; (b) **4,4'-BPS@(β -CD)₂**, and (c) **2,4'-BPS@ β -CD** at 25°C in neutral aqueous solution.

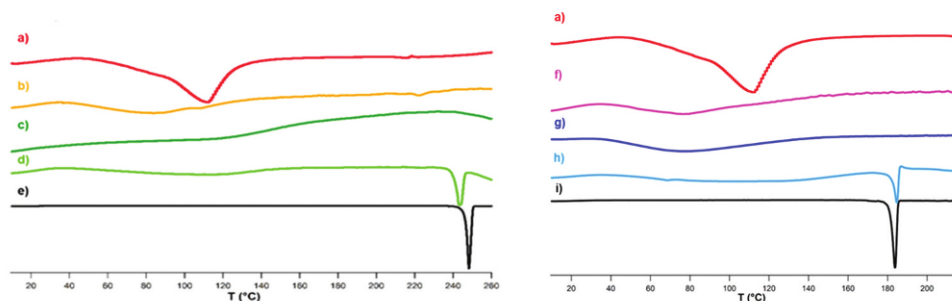


Figure 9. DSC curves. (Left) (a) β -CD; (b-d) 1:2, 1:1, and 2:1 mixtures of 4,4'-BPS and β -CD (e) 4,4'-BPS. (Right) (a) β -CD; (f-h) 1:2, 1:1, and 2:1 mixtures of 2,4'-BPS and β -CD. (i) 2,4'-BPS.

CD, while for the molar ratio of 1:2 there is the evidence that not all the 4,4'-BPS was included inside the β -CD-cavity (Figure 9d) [50,51].

DSC analysis of the mixtures β -CD/2,4'-BPS at different molar ratios shows analogous features. The formation of the 2,4'-BPS@ β -CD inclusion complex was highlighted by the disappearance of the endothermic peaks attributable to the free 2,4'-BPS and β -CD starting materials. In detail, the 1:1 and 2:1 mixtures β -CD/2,4'-BPS (Figures 9g and 9f, respectively) showed weak and broad curves from 50°C to 110°C associated with the release of residual water from the β -CD cavity or in the crystal packing. The sharp and endothermic peak of the pure 2,4'-BPS (melting event, $T_{\max} = 183.7^\circ\text{C}$), is also detected in the DSC curve of the 1:2 β -CD/2,4'-BPS mixture (Figure 9h).

Thermogravimetric analysis (TGA, SI) of the BPS@ β -CD inclusion complexes was also carried out. Free β -CD shows a first mass elimination from room temperature up to 105°C: this 11% w/w mass loss is attributed to the evaporation of both surface water and internal water associated with the macrocycle. The β -CD thermic degradation starts at 304.3°C (SI) (second mass elimination). Furthermore, for 4,4'-BPS raw material, it is possible to observe (SI) a first degradation process starting at 307.8°C where the mass of the molecule is reduced by about 85%. Differently, for 2,4'-BPS isomer, the mass reduction starts at a lower temperature ($T = 239.3^\circ\text{C}$, see SI). Thermogravimetric curves (SI) of 1:1 mixtures BPS/ β -CD show distinct features with respect to the free components. In detail, for both 4,4'-BPS/ β -CD and 2,4'-BPS/ β -CD mixtures the event at $T < 105^\circ\text{C}$ attributable to the loss of water is strongly reduced, in accordance with DSC results. In addition, the degradation temperature of both BPS@ β -CD complexes starts at slightly lower $T(^{\circ}\text{C})$ than those of the starting raw materials (SI), clearly showing that no thermal stabilisation of 4,4'-BPS and 2,4'-BPS-based complexes occurs upon inclusion inside the β -CD cavity. Furthermore, there is

no evidence of free 4,4'-BPS and 2,4'-BPS in 1:1 BPS/ β -CD mixtures, confirming that both guests are completely included into the cyclodextrin cavity.

Conclusion

In conclusion, we have here characterised and described the formation of inclusion complexes between β -CD host and the two isomeric 4,4'-dihydroxydiphenyl sulphone and 2,4'-dihydroxydiphenyl sulphone (BPSs), in solution, in the gas phase, and in the solid state. In solution, the formation of the inclusion complexes 4,4'-BPS@ β -CD and 2,4'-BPS@ β -CD was shown by 1D and 2D NMR (NOESY and DOSY) experiments, while ITC investigation evidenced that the β -CD host shows a greater affinity for 4,4'-BPS with respect to its isomer 2,4'-BPS, with a 4,4'-BPS/2,4'-BPS selectivity ratio of 6.3. ITC clearly shows that the formation of the 1:1 species is enthalpically driven but accompanied by an unfavourable entropic change. The formation of the inclusion complexes between the β -CD and the two isomeric 4,4'-BPS and 2,4'-BPS was detected also in the gas phase by FT ICR ESI MS studies. In the gas phase, collision-induced dissociation experiments indicate that 4,4'-BPS has a higher kinetic barrier to escape from the β -CD cavity than the isomeric 2,4'-BPS. In the solid state, the 4,4'-BPS@ β -CD complex forms a head-to-head dimer constituted by two β -CD macrocycles, which hosts two 4,4'-BPS guests. The dimer of β -CD is sealed by seven strong H-bonding interactions involving exclusively the secondary O3 hydroxyl groups. Analogously, the 2,4'-BPS@ β -CD complex forms a tubular dimeric assembly in the solid state in which two 2,4'-BPS guests are included in the cavity. In the solid state, the inclusion of the 4,4'-BPS guest inside the β -CD cavity results in the entrapment of some water molecules at the dimeric interface. Finally, the formation of inclusion complexes between 4,4'-BPS or 2,4'-BPS and β -CD was also confirmed by FT IR, DSC, and TGA

analysis. DSC curves evidenced significant changes in material properties of **4,4'-BPS@ β -CD** and **2,4'-BPS@ β -CD** complexes in comparison to the starting raw materials; unexpectedly, no thermal stabilisation was detected by TGA analysis for both **4,4'-BPS** and **2,4'-BPS** upon inclusion inside the **β -CD** cavity.

Experimental section

General methods

HR ESI mass spectra were recorded on a FT-ICR mass spectrometer equipped with a 7 T magnet. The samples were ionised in positive ion mode using ESI positive mode. The mass spectra were calibrated externally, and a linear calibration was applied. All chemicals of reagent grade were used as purchased without further purification. The two isomers 4,4'-dihydroxydiphenyl and 2,4'-dihydroxydiphenyl sulphones were purchased from TCI (GC grade > 98%) and was also used without further purification. The β -cyclodextrin (β -CD) was obtained from Roquette (Kleptose® GC grade \geq 93%) and used after being dried by freeze-drying. Reaction temperatures were measured externally. NMR spectra were recorded on a 600 MHz spectrometer [600 (^1H) and 150 MHz (^{13}C)], 400 [400 (^1H) and 100 MHz (^{13}C)] and 300 [300 (^1H) and 75 MHz (^{13}C)]. Chemical shifts are reported relatively to the residual solvent peak. DOSY experiments were performed on a Bruker 400 spectrometer equipped with 5 mm PABBO BB| 19 F-1H\|D Z-GRD Z114607/0109. The standard Bruker pulse program, ledbp2s, employing a double stimulated echo sequence and LED, bipolar gradient pulses for diffusion, and two spoil gradients was utilised. Individual rows of the quasi-2D diffusion databases were phased, and the baseline was corrected.

FT IR spectra in the medium infrared region (MIR) were obtained with a 4100 Type A spectrometer (JASCO Europe) equipped with a triglycine sulphate (TGS) detector at a resolution of 4 cm^{-1} . MIR measurements were derived by averaging 1000 scans obtained on samples dispersed in anhydrous KBr tablets. Baseline correction was performed with the Jasco FT-IR spectrometer software.

Thermogravimetric analysis was carried out with a TGA Q500 thermobalance (TA Instruments). A working N_2 flux of $100\text{ cm}^3/\text{min}$ was used. The TG profile was recorded in the $25 < T\text{ (}^\circ\text{C)} < 900$ temperature range, using open platinum pans loaded with ca. 7 mg of each sample. The heating rate was of $10^\circ\text{C}/\text{min}$. The balance resolution is $1\text{ }\mu\text{g}$.

Differential Scanning Calorimetry (DSC) measurements were carried out with a DSC 25P Scanning Calorimeter (TA Instrument). Measurements were carried out with a heating rate of $10^\circ\text{C}/\text{min}$ in the $5 < T\text{ (}^\circ\text{C)} < 260$ temperature range on ca. 5 mg of a sample hermetically sealed in an aluminium pan.

Calorimetric titrations (ITCs) were carried out at 25°C with a nano-isothermal titration calorimeter Nano-ITC (TA Instruments, USA) having an active cell volume of 0.988 mL and a 250 μL injection syringe. The reaction mixture in the sample cell was continuously stirred at 250 rpm during the titration. Measurements were run in the overfilled mode, which does not require any correction for liquid evaporation and for the presence of the vapour phase [52]. The power curve was integrated with NanoAnalyze software (TA Instruments, USA) to obtain the gross heat evolved/absorbed in the reaction. The instrument was calibrated chemically using a test HCl/TRIS reaction following the procedure previously described [53] and was also checked by running an electrical calibration.

Calorimetric experiments were carried out by titrating a 4,4'-dihydroxydiphenyl sulphone (**4,4'-BPS**) or a 2,4'-dihydroxydiphenyl sulphone (**2,4'-BPS**) solution (0.2–0.5 mM) with an aqueous solution of **β -CD** (4–5 mM).

Both **β -CD** and guests were dissolved in 50 mM phosphate buffer (pH 7). The buffer was chosen to minimise any contribution resulting from the interaction of the reactants with the proton. Before each experiment, all the solutions were degassed and stirred under vacuum for about 15 minutes. Typically, 4–5 independent titrations were run for each **β -CD** – guest system to explore both smaller (about 2.5) and larger (up to 6) host/guest ratios and thus collect a suitable number of points to investigate the possible formation of multiple species; the two sets of curves were refined together to obtain the final parameters. The heats of dilution were determined in separate blank experiments by titrating a solution containing phosphate buffer only with solutions of **β -CD** (prepared in phosphate buffer).

The net heat of the reaction, obtained by subtracting the heat evolved/absorbed in the blank experiments, was treated by HypCal [54], a software that allows for the determination of equilibrium constants and formation enthalpies of complex species in solution by a non-linear least-squares analysis of calorimetric data. Thermodynamic parameters were determined by handling simultaneously data obtained from different titrations.

Inclusion complexes formation

The synthesis of **BPS@ β -CD** pseudorotaxane complexes was conducted in a flask under atmospheric pressure. **β -CD** (9.0 mg, 8.0×10^{-3} mmol) was solubilised in 10 mL of deionised water. Then, an appropriate amount of the **BPS** guest was added (1.8 mg, 8.0×10^{-3} mmol), and the resulting mixture was stirred at 25°C for 30 min. Finally, the water was evaporated under vacuum, and the product was further dried and stored at room temperature. **^1H NMR** (400 MHz, 298 K, D_2O) of the equimolar mixture of **β -CD** and **4,4'-BPS** (3.0 mM); δ 7.71 (H_2^{G} , d, $J = 8.8$ Hz, 4H), 6.97 (d, H_1^{G} , $J = 8.8$ Hz, 4H), 5.00 (H_1 , d, $J = 3.6$ Hz, 7 H), 3.83 (dd, H_3 , $J_1 = J_2 = 9.5$ Hz, 7 H), 3.74 (d, H_6 , $J = 2.0$ Hz, 14 H), 3.60 (dd, H_2 , $J_1 = 9.9$ Hz, $J_2 = 3.6$ Hz, 7 H), 3.53 (dd, H_4 , $J_1 = J_2 = 9.0$ Hz, 7 H), 3.47–3.44 (broad, H_5 , 7 H). **^{13}C NMR** (75 MHz, 298 K, D_2O): 162.0, 132.1, 129.4, 116.6, 102.3, 81.3, 73.6, 72.4, 72.2, 60.2. **HRMS (ESI)**: m/z [**4,4'-BPS@ β -CD** + 2Na] $^{2+}$ calculated for $\text{C}_{54}\text{H}_{80}\text{Na}_2\text{O}_{39}\text{S}$, 715.1891; found: 715.1881. **^1H NMR** (600 MHz, 298 K, D_2O) of the equimolar mixture of **β -CD** and **2,4'-BPS** (3.0 mM); δ 7.89 (H_1^{G} , dd, $J_1 = 8.4$ Hz, $J_2 = 1.8$ Hz, 1 H), 7.81 (d, H_5^{G} , $J = 8.8$ Hz, 2 H), 7.62 (ddd, H_3^{G} , $J_1 = J_2 = 8.0$ Hz, $J_3 = 1.7$ Hz, 1 H), 7.17 (dd, H_2^{G} , $J_1 = J_2 = 7.8$ Hz, 1 H), 7.06 (d, H_4^{G} , $J = 8.4$ Hz, 1 H), 6.92 (d, H_6^{G} , $J = 8.8$ Hz, 2 H), 5.04 (H_1 , d, $J = 3.7$ Hz, 7 H), 3.89 (dd, H_3 , $J_1 = J_2 = 9.3$ Hz, 7 H), 3.81 (d, H_6 , $J = 2.7$, 14 H), 3.65–3.62 (overlapped, H_2 + H_4 , 14 H), 3.57 (broad, H_5 , 7 H). **^{13}C NMR** (75 MHz, 298 K, D_2O): 162.7, 155.9, 137.5, 132.4, 130.6, 129.7, 126.6, 121.8, 119.4, 116.7, 102.9, 82.2, 74.2, 73.2, 72.9, 61.2. **HRMS (ESI)**: m/z [**2,4'-BPS@ β -CD** + 2Na] $^{2+}$ calculated for $\text{C}_{54}\text{H}_{80}\text{Na}_2\text{O}_{39}\text{S}$, 715.1891; found: 715.1887.

Job's plot

Stock solutions of **β -CD** (2.66 mM) and **4,4'-BPS** (2.66 mM) in water were prepared. 5-mm NMR tubes were filled with 500 μL solutions of **β -CD** and **4,4'-BPS** in the following volume ratios: 50/450, 100/400, 150/350, 200/300, 250/250, 300/200, 350/150, 400/100, 450/50, 500/0 ($\mu\text{L}/\mu\text{L}$). The chemical shift of H_3 -atom of **β -CD** was recorded for each sample, and the corresponding concentration of the complex was determined. The Job's plot was obtained by plotting the complex concentration as a function of the mole fraction of **β -CD**.

Determination of the crystallographic structures of 4,4'-BPS@ β -CD and 2,4'-BPS@ β -CD

Single crystals of **4,4'-BPS@ β -CD** and **2,4'-BPS@ β -CD** suitable for X-ray diffraction structure analysis were obtained by evaporation of aqueous solutions containing 1:1 molar mixtures of **β -CD** and the **4,4'-BPS** or **2,4'-BPS** guest molecules. Data collection was carried out at

the Macromolecular crystallography XRD1 beamline of the Elettra synchrotron (Trieste, Italy), employing the rotating-crystal method with a Dectris Pilatus 2 M area detector. Single crystals were dipped in paratone cryo-protectant, mounted on a nylon loop and flash-frozen under a nitrogen stream at 100 K. Diffraction data were indexed and integrated using the XDS package [55], while scaling was carried out with XSCALE [56]. Structures were solved using the SHELXT program [57] and structure refinement was performed with SHELXL-18/3 [58], operating through the WinGX GUI [59], by full-matrix least-squares (FMLS) methods on F^2 . Non-hydrogen atoms were refined anisotropically, except some disordered groups with low occupancy factors. Hydrogen atoms were added at the calculated positions and refined using the riding model. Crystallographic data are reported in Table S1.

Acknowledgments

The authors thank the Regione Campania for the PhD Grant "Dottorati di Ricerca con Caratterizzazione Industriale" DGR n. 156 del 21/03/2017 P.O.R. CAMPANIA FSE 2014/2020 – ASSE III – Obiettivo Specifico 14 Azione 10.4.5: POR D44J18000310006. The authors thank the Regione Campania (POR CAMPANIA FESR 2007/2013 O.O.2.1, B46D14002660009, "Il potenziamento e la riqualificazione del sistema delle infrastrutture nel settore dell'istruzione, della formazione e della ricerca"), for the FT-ICR mass spectrometer facilities, the Centro di Tecnologie Integrate per la Salute (CITIS, Project PONA3_00138), Università di Salerno, for the 600 MHz NMR facilities.

Disclosure statement

No potential conflict of interest was reported by the author(s).

Funding

This work was supported by the Regione Campania [B46D14002660009, POR D44J18000310006].

ORCID

Carmen Talotta  <http://orcid.org/0000-0002-2142-6305>
Silvano Geremia  <http://orcid.org/0000-0002-0711-5113>
Neal Hickey  <http://orcid.org/0000-0003-1271-5719>
Carmine Gaeta  <http://orcid.org/0000-0002-2160-8977>
Placido Neri  <http://orcid.org/0000-0003-4319-1727>

Supporting information

X-ray details, and tables of crystal data, Job's plot, DOSY experiments, TGA and FT IR spectra. This material is available free of charge via the Internet at <http://www.tandfonline.com>.

- [1] Klemes MJ, Skala LP, Ateia M, et al. polymerized molecular receptors as adsorbents to remove micropollutants from water. *Acc Chem Res.* **2020**;53:2314–2324.
- [2] Ling Y, Klemes MJ, Xiao L, et al. Benchmarking micropollutant removal by activated carbon and porous β -cyclodextrin polymers under environmentally relevant scenarios. *Environmental Science & Technology.* **2017**;51:7590–7598.
- [3] Schwarzenbach RP, Escher BI, Fenner K, et al. The challenge of micropollutants in aquatic systems. *Science.* **2006**;313:1072–1077.
- [4] Long A, Lefevre S, Guy L, et al. Recognition of the persistent organic pollutant chlordecone by a hemicyclopentane cage. *New J Chem.* **2019**;43:10222–10226.
- [5] Morin-Crini N, Crini G. Environmental applications of water-insoluble β -cyclodextrin-epichlorohydrin polymers. *Prog Polym Sci.* **2013**;38:344–368.
- [6] Lo Meo P, Lazzara G, Liotta L, et al. Cyclodextrin-calixarene co-polymers as a new class of nanosponges. *Polym Chem.* **2014**;5:4499–4510.
- [7] Thoene M, Rytel L, Nowickac N, et al. The state of bisphenol research in the lesser developed countries of the EU: a mini-review. *Toxicol Res.* **2018**;7:371–380.
- [8] Chen D, Kannan K, Tan H, et al. bisphenol analogues other than BPA: environmental occurrence, human exposure, and toxicity-a Review. *Environ Sci Technol.* **2016**;50:5438–5453.
- [9] Fang Z, Gao Y, Wu X, et al. A critical review on remediation of bisphenol S (BPS) contaminated water: efficacy and mechanisms. *Crit Rev Env Sci Tec.* **2020**;50:476–522.
- [10] Vandenberg LN, Hauser R, Marcus M, et al. Human exposure to bisphenol A (BPA). *Reprod Toxicol.* **2007**;24:139–177.
- [11] Wu LH, Zhang XM, Wang F, et al. Occurrence of bisphenol S in the environment and implications for human exposure: a short review. *Sci Total Environ.* **2018**;615:87–98.
- [12] Crump D, Chiu S, Williams KL. Bisphenol S alters embryonic viability, development, gallbladder size, and messenger RNA expression in chicken embryos exposed via egg injection. *Environ Toxicol Chem.* **2016**;35:1541–1549.
- [13] Beronius A, Ruden C, Hakansson H, et al. Risk to all or none? A comparative analysis of controversies in the health risk assessment of Bisphenol A, *Reprod. Toxicol.* **2010**;29:132–146.
- [14] Shabtai IA, Mishaal YA. Polycyclodextrin-clay composites: regenerable dual-site sorbents for bisphenol a removal from treated wastewater. *ACS Appl Mater Interfaces.* **2018**;10:27088–27097.
- [15] Alsbaiee A, Smith BJ, Xiao L, et al. Rapid removal of organic micropollutants from water by a porous β -cyclodextrin polymer. *Nature.* **2016**;529:190–194.
- [16] Li G, Beibei W, Feng W, et al. Effects of cyclodextrin on photodegradation of 4, 4'-sulfonyldiphenol in aqueous solution. *Res J Chem Environ.* **2011**;15:13–16.
- [17] Kitano H, Endo H, Gemmei-Ide M, et al. inclusion of bisphenols by cyclodextrin derivatives. *J Incl Phenom Macrocycl Chem.* **2003**;47:83–90.
- [18] Nakaji-Hirabayashi T, Endo H, Kawasaki H, et al. Inclusion of bisphenols by a self-assembled monolayer of thiolated calix[6]arene on a gold surface. *Environ Sci Technol.* **2005**;39:5414–5420.
- [19] Kadam VV, Balakrishnan RM, Ettiyappan JP. Fluorometric detection of bisphenol A using β -cyclodextrin-functionalized ZnO QDs. *Environ Sci Pollut Res.* **2021**;28:11882–11892.
- [20] Ye Z, Wang Q, Qiao J, et al. Simultaneous detection of bisphenol A and bisphenol S with high sensitivity based on a new electrochemical sensor. *J Electroanal Chem.* **2019**;854:113541–113550.
- [21] Szejtli J. Introduction and general overview of cyclodextrin chemistry. *Chem Rev.* **1998**;98:1743–1753.
- [22] Crini G. A History of Cyclodextrins. *Chem Rev.* **2014**;114:10940–10975.
- [23] Vegter GC, de Brabander MM. Separation and purification of isomeric dihydroxydiphenyl sulfones. *US Patent 3065274*, Nov. 20, **1962**.
- [24] Gaeta C, Talotta C, Farina F, et al. Conformational features and recognition properties of a conformationally blocked calix[7]arene derivative. *Chem Eur J.* **2012**;18:1219–1230.
- [25] Gaeta C, Talotta C, Neri P. Pseudorotaxane orientational stereoisomerism driven by π -electron density. *Chem Commun.* **2014**;50:9917–9920.
- [26] Hirose K. A practical guide for the determination of binding constants. *J Incl Phenom Macrocyclic Chem.* **2001**;39:193–209.
- [27] Hirose K. In analytical methods in supramolecular chemistry. Weinheim: Wiley-VCH; **2007**.
- [28] Cohen Y, Avram L, Frish L. Diffusion NMR spectroscopy in supramolecular and combinatorial chemistry: an old parameter-new insights. *Angew Chem Int Ed.* **2005**;44:520–554.
- [29] Timmerman P, Weidmann JL, Jolliffe KA, et al. NMR diffusion spectroscopy for the characterization of multi-component hydrogen-bonded assemblies in solution. *J Chem Soc Perkin Trans.* **2000**;2:2077–2089.
- [30] Gaeta C, Caruso T, Mincoletti M, et al. p-Sulfonatocalix[7]arene: synthesis, protolysis, and binding ability. *Tetrahedron.* **2008**;Vol. 64:5370–5378.
- [31] Della Sala P, Talotta C, Caruso T, et al. Tuning cycloparaphenylene host properties by chemical modification. *J Org Chem.* **2017**;82:9885–9889.
- [32] Del Regno R, Della Sala P, Spinella A, et al. Calix[2]naphtha[2]arene: a class of naphtharene-phenol hybrid macrocyclic hosts. *Org Lett.* **2020**;22:6166–6170.
- [33] Betlejewska-Kielak K, Bednarek E, Budzianowski A, et al. comprehensive characterisation of the ketoprofen- β -cyclodextrin inclusion complex using x-ray techniques and NMR spectroscopy. *Molecules.* **2021**;26:4089–4110.
- [34] Talotta C, Gaeta C, Qi Z, et al. Pseudorotaxanes with self-sorted sequence and stereochemical orientation. *Angew Chem Int Ed.* **2013**;52:7437–7441.
- [35] Baytekin B, Baytekin TH, Schalley CA. Mass spectrometric studies of non-covalent compounds: why supramolecular chemistry in the gas phase. *Org Biomol Chem.* **2006**;4:2825–2841.
- [36] Schalley CA. Molecular recognition and supramolecular chemistry in the gas phase. *Mass Spectrom Rev.* **2001**;20:253–309.

- [37] Weimann DP, Kogej M, Schalley CA. In mass spectrometry and gas phase chemistry of supramolecules, analytical methods in supramolecular chemistry. Weinheim: Wiley-VCH; **2012**.
- [38] Cunniff JB, Vouros P, Desiderio DM. Mass and charge assignment for electrospray ions by crown ether adduction. *Rapid Commun Mass Spectrom*. **1994**;8:715–719.
- [39] For a review on cyclodextrins in the gas phase, see: Lebrilla CB. The gas-phase chemistry of cyclodextrin inclusion complexes. *Acc Chem Res*. **2001**;34:653–661.
- [40] Yang ZX, Chen Y, Liu Y. Inclusion complexes of bisphenol A with cyclomaltoheptaose (β -cyclodextrin): solubilization and structure. *Carbohydr Res*. **2008**;343:2439–2442.
- [41] Makedonopoulou S, Mavridis IM. Structure of the inclusion complex of β -cyclodextrin with 1,12-dodecanedioic acid using synchrotron radiation data; a detailed dimeric β -cyclodextrin structure. *Acta Cryst*. **2000**;B56:322–331.
- [42] Bonaccorso C, Brancatelli G, Forte G, et al. Factors driving the self-assembly of water-soluble calix[4]arene and gemini guests: a combined solution, computational and solid-state study. *RSC Adv*. **2014**;4:53575–53587.
- [43] Bonaccorso C, Migliore R, Volkova M, et al. Self-assembling of supramolecular adducts by sulfonato-calix[4]arene and pyridinium gemini guests in neutral aqueous solution. *Thermochim Acta*. **2017**;656:47–52.
- [44] Guo DS, Uzunova VD, Assaf KI, et al. Inclusion of neutral guests by water-soluble macrocyclic hosts - a comparative thermodynamic investigation with cyclodextrins, calixarenes and cucurbiturils. *Supramol Chem*. **2016**;28:384–395.
- [45] Wang Z, Landy D, Sizun C, et al. Cyclodextrin complexation studies as the first step for repurposing of chlorpromazine. *Int J Pharm*. **2020**;584:119391–119405.
- [46] Cai C, Liu M, Yan H, et al. A combined calorimetric, spectroscopic, and molecular dynamic simulation study on the inclusion complexation of (E)-piceatannol with hydroxypropyl- β -cyclodextrin in various alcohol + water cosolvents. *J Chem Thermodyn*. **2019**;132:341–351.
- [47] Saha S, Roy A, Roy K, et al. Study to explore the mechanism to form inclusion complexes of β -cyclodextrin with vitamin molecules. *Sci Rep*. **2016**;6:1–12.
- [48] Matencio A, Navarro-Orcajada S, García-Carmona F, et al. Applications of cyclodextrins in food science. A review. *Trends Food Sci Technol*. **2020**;104:132–143.
- [49] Campoy AV, Freire E. ITC in the post-genomic era ...? priceless. *Biophys Chem*. **2005**;115:115–124.
- [50] Liu H, Cai X, Wang Y, et al. Adsorption mechanism-based screening of cyclodextrin polymers for adsorption and separation of pesticides from water. *Water Res*. **2011**;45:3499–3511.
- [51] Abarca RL, Rodríguez FJ, Guarda A, et al. Characterization of beta-cyclodextrin inclusion complexes containing an essential oil component. *Food Chem*. **2016**;196:968–975.
- [52] Hansen LD, Fellingham GW, Russell DJ. Simultaneous determination of equilibrium constants and enthalpy changes by titration calorimetry: methods, instruments, and uncertainties. *Anal Biochem*. **2011**;409:220–229.
- [53] Sgarlata C, Zito V, Arena G. Conditions for calibration of an isothermal titration calorimeter using chemical reactions. *Anal Bioanal Chem*. **2013**;405:1085–1094.
- [54] Arena G, Gans P, Sgarlata C. HypCal, a general-purpose computer program for the determination of standard reaction enthalpy and binding constant values by means of calorimetry. *Anal Bioanal Chem*. **2016**;408:6413–6422.
- [55] Xds KW. *Acta Crystallogr. Sect D: Biol Crystallogr*. **2010**;66:125–132.
- [56] Kabsch W. Integration, scaling, space-group assignment and post-refinement. *Acta Crystallogr D Biol Crystallogr*. **2010**;66:133–134.
- [57] Sheldrick GM. Integrated space-group and crystal-structure determination. *Acta Cryst Section A*. **2015**;71:3–8.
- [58] Sheldrick GM. A short history of SHELX. *Acta Cryst Section A*. **2008**;64:112–122.
- [59] WinGX FL. ORTEP for windows: an update. *J Appl Cryst*. **2012**;45:849–854.

Copyright of Supramolecular Chemistry is the property of Taylor & Francis Ltd and its content may not be copied or emailed to multiple sites or posted to a listserv without the copyright holder's express written permission. However, users may print, download, or email articles for individual use.